TREE SPECIES CLASSIFICATION USING HYPERSPECTRAL IMAGERY: A COMPARISON OF TWO CLASSIFIERS

A thesis submitted to the faculty of
San Francisco State University
In partial fulfillment of
the requirements for
the Degree

Master of Arts

In

Geography

by

Laurel Rainie Ballanti

San Francisco, California

January 2016

CERTIFICATION OF APPROVAL

I certify that I have read Tree Species Classification Using Hyperspectral Imagery: A Comparison of Two Classifiers by Laurel Rainie Ballanti, and that in my opinion this work meets the criteria for approving a thesis submitted in partial fulfillment of the requirement for the degree Master of Arts in Geography at San Francisco State University.

Leonhard Blesius, Ph.D
Professor of Geography

Ellen Hines, Ph.D
Professor of Geography

Bill Kruse
Consultant, Kruse Imaging

TREE SPECIES CLASSIFICATION USING HYPERSPECTRAL IMAGERY: A COMPARISON OF TWO CLASSIFIERS

Laurel Rainie Ballanti
San Francisco, California
2016

The use of hyperspectral and LiDAR data for tree species classification can be a useful and efficient tool of forest managers for planning and monitoring purposes. The first objective of this research was to create a high accuracy species map to be used in a tree inventory of Muir Woods National Monument and Kent Creek Canyon in Marin County, California. Secondly, a comparative classification approach was used to test the performance of two non-parametric classifiers, support vector machines (SVM) and random forest (RF), in classifying eight tree species, including old growth redwood, found in the steep terrain of the study area. A minimum noise fraction transform was applied to the hyperspectral imagery to reduce data dimensionality and a LiDAR derived canopy height model provided the basis for the object-oriented classification. The influence of training sample size and segmentation size on the classifications was also explored further. Both classifiers were compared together and individually. SVM outperformed RF in overall accuracy (OA) in all comparisons, however, the statistical significance of the improved accuracy was varied. All classifications resulted in high overall accuracies above 90%.

I certify that the Abstract is a correct representation of the content of this thesis.

L. Ballanti — 5.11.15

Chair, Thesis Committee — Date

ACKNOWLEDGEMENTS

Thanks is given to my committee members, Leonhard Blesius, Ellen Hines, and Bill Kruse for their encouragement and guidance on this research. This research was supported by the Golden Gate National Recreational Area and California State Parks. Additional thanks is given to Nathan Grieg and the Romberg Tiburon Center for Environmental Studies for their assistance and support. Lastly, I thank Ananda Bhattacharya for his help with programming, field work, and support throughout this research.

TABLE OF CONTENTS

LIST OF TABLES

LIST OF FIGURES

Figures Page

LIST OF APPENDICES

Appendix Page

1. Introduction

The identification of trees species through remote sensing provides an efficient and potentially cost-effective way to inventory, protect, and manage forest resources (Leckie et al., 2005; Dalponte et al., 2008; Peerbhay et al., 2013; Ghosh et al. 2014; Franklin, 2001). Detailed and accurate forest maps are crucial for preparation and monitoring of fire, drought, and other forest disturbances caused by climate change (Daplonte et al., 2008; Franklin, 2010; Dale et al., 2001). Remotely-sensed images contain pixels displaying different surface objects with unique reflectance values, allowing for the discrimination of classes, such as trees and vegetation, based on their spectral signatures (Landgrebe, 2002). Forest classifications have ranged from more general classifications of forest type (deciduous and coniferous trees) (Gislason et al., 2006; Ghosh et al., 2014) to narrower focus classifications of single tree species (Van Aardt & Wynne, 2007; Martin et al., 1998; Leckie et al., 2005). Often, the ability to classify individual species is limited, due to the lack of spectral variance, which helps discriminate small spectral differences between species (Clark et al., 2005).

The type of imagery is a major factor in classification analysis, as the spatial and spectral resolution can influence the accuracy of a classification. Often multispectral images with three to eight bands are commonly used with land-cover classifications or forest type (broadleaf, conifer) identification (Gislason et al., 2006; Akar & Gungar, 2013; Clark et al., 2005). In some cases, the limited spectral bands available with

multispectral imagery are combined with additional data, including LiDAR, tree heights, shape (Holmgren et al., 2008; Dalponte et al., 2012), multi-temporal imagery (Key et al., 2001), and texture (Franklin et al., 2000).

Hyperspectral images contain multiple (typically between 64 and 256) continuous narrow bands, providing significant levels of detail which allow for the distinction of fine spectral variations among tree species (Shippert, 2004). Despite the abundance of information contained in hyperspectral imaging, discriminating species within the same genus can be a challenge, often leading to misclassification (Peerbhay et al., 2013; Heinzel & Koch, 2012). However, in a comparison between hyperspectral and simulated broadband multispectral classifications in tropical tree species, Clark et al. (2005) found that hyperspectral significantly outperformed multispectral. Where multispectral fails to capture the slight spectral differences which occur between tree species, data-rich hyperspectral imagery can improve classifications by providing sufficient information to discriminate between spectrally similar targets (Clark et al., 2005; Dalponte et al., 2012). This has resulted in the extensive use of hyperspectral imagery for tree species classifications (Van Aardt and Wynne, 2007; Tarabalka et al., 2010; Ghosh et al., 2014; Jones et al., 2010).

The high level of data dimensionality in hyperspectral imagery poses a problem for classifications due to the Hughes Phenomenon (Hughes, 1968). The increase in spectral bands associated with hyperspectral imagery changes the ratio between the

number of training samples and the number of bands, causing the accuracy of the classifier to decrease (Melgani & Bruzzone, 2004). To resolve this issue data reduction through band selection reduces dimensionality without the need to increase training samples (Clark et al., 2005). One common method of feature selection in recent years has been the minimum noise fraction (MNF) (Tarabalka et al., 2010; Denghui & Le, 2011; Rojas et al., 2010; Voss & Sugumaran, 2008; Buddenbaum et al., 2005; Ghosh et al., 2014). The MNF is a transformation based on two principal component analysis rotations, which first uses principal components to de-correlate noisy data, and secondly uses the noise-removed principal components for the final transformation (ENVI 2013). Resulting MNF bands are ranked by eigenvalue from those containing highest variance to highest noise.

Image analysis using pixel-based approaches have been popular (Xiao et al., 2004; Dalponte et al., 2008; Buddenbaum et al., 2005), although challenges with this approach have been identified. Issues with pixel-level analysis include shadowed or noise-filled pixels (Dalponte el al., 2014), mixed pixels, or for very high resolution imagery, high spectral variety within a class (Alonzo et al., 2014).

Object-oriented tree segmentation for tree species classifications commonly occurs on the individual tree crown level (Clark et al., 2005; Heinzel & Koch, 2012). Dalponte et al. (2014) tested delineation methods with both airborne laser scanning (ALS) and hyperspectral data, and determined that neither method was significantly

better than the other. When compared with the pixel-based approach, object-based methods have been shown to provide improved classification accuracy in many cases Voss & Sugumaran, 2008; Van Aardt & Wynne, 2007; Tarabalka et al., 2010; Clark et al., 2005).

The support vector machine (SVM) classifier has been increasingly used for complex multi-class problems because it has been found to be better prepared to handle highly dimensional data without an increase in training sample size (Mountrakis et al., 2011) and some authors even suggest that data reduction is unnecessary for such classifiers (Ghosh et al., 2014). The wide use of the SVM classifier has been apparent in both land-cover (forest type) classifications (Tarabalka et al., 2010; Denghui & Le, 2011; Rojas et al., 2010) and tree species classifications (Dalponte et al., 2014; Heinzel & Koch, 2012; Jones et al., 2010), making it one of the more common classifiers used in vegetation classifications.

Support vector machines contain a machine learning algorithm which separates classes by defining an optimal hyperplane between classes, based on support vectors which are defined by training data (Mountrakis et al., 2011). At its most basic form, a SVM is a linear binary classifier, however multi-class strategies have been created which can be applied to complex hyperspectral classifications (Melgani & Bruzzone, 2004). While the SVM classifier is seen as a robust method which requires only a small training sample size, the classifier requires trial and error tuning to determine parameters for each

classification (Mountrakis et al., 2011). The nonlinear SVM with radial basis kernel functions (RBF) requires two parameters to be set. The C parameter determines the amount of misclassification allowed for non-separable training data, enabling the rigidity of training to be adjusted (Exelis Visual Information Solutions 2013). The gamma parameter is a kernel width parameter which determines smoothing of the shape of the class dividing hyperplane (Melgani & Bruzzone, 2004).

Another non-parametric classifier gaining wider use is the random forest classifier (RF) as developed by Breiman (2001). Random forest is an ensemble-based machine learning algorithm which uses multiple decision tree classifiers to vote on a final classification. Only a few parameters are required, including N (number of trees) and m (number of predictor features) (Akar & Gungor, 2013). With minimal parameter setting and few variables, random forest has been found to require less complex computations and running time than other classifiers, as well as having high classification accuracy in especially intricate models (Cutler et al., 2007). Random forest has been suggested as an alternate classifier to SVM for multi-class problems, as it requires fewer parameters than SVM (Akar & Gungor, 2013).

There are two objectives of this research. First, to use LiDAR and hyperspectral imagery to increase the accuracy of forest species mapping in a complex forest. Secondly, to compare and examine the performance of two state-of-the-art classifiers: random forests and support vector machines for tree species classification in a forest

setting with non-homogenous tree species distribution. A comparative classification approach is used to assess the performance of the two classifiers, with additional consideration for influence of training sample size and object-based segmentation size.

2. Study Area

The study area consists of Muir Woods National Monument and adjacent Kent Creek Canyon, located in Marin County, CA, about 15 miles north of San Francisco, CA (Figure 1). The parks are managed by the U.S. National Parks Service and the California State Parks, respectively. Both parks occur within the Redwood Creek watershed, which extends steeply to the Pacific Ocean, roughly 5.5 miles to the south. The park's close proximity to the colder ocean water creates fog, resulting in fog drip which helps support the redwood forest ecosystem (Schoenherr, 1992). In 1908, Muir Woods became a National Monument, protecting the remaining old growth redwoods. With over 1 million visitors in 2014, efforts within Muir Woods are being made to minimize high visitor impacts, including erosion, noise-pollution, and traffic. (National Parks Conservation Association, 2011; National Park Service, 2014).

Muir Woods National Monument occupies 2.25 square kilometers in the upper reaches of the Redwood Creek Watershed, where old growth coast redwoods (*Sequoia sempervirens*), Douglas fir (*Pseudotsuga menziesii*), and California bay laurel (*Umbellularia californica*) dominate the forest canopy. The extent of tan oak (*Lithocarpus densiflorus*) and big leaf maple (*Acer macrophyllum*) are limited, but occupy both canopy and understory. Although some of the redwood trees in the area are over 600 years old, the forest contains trees of varying ages (National Park Service, 2008).

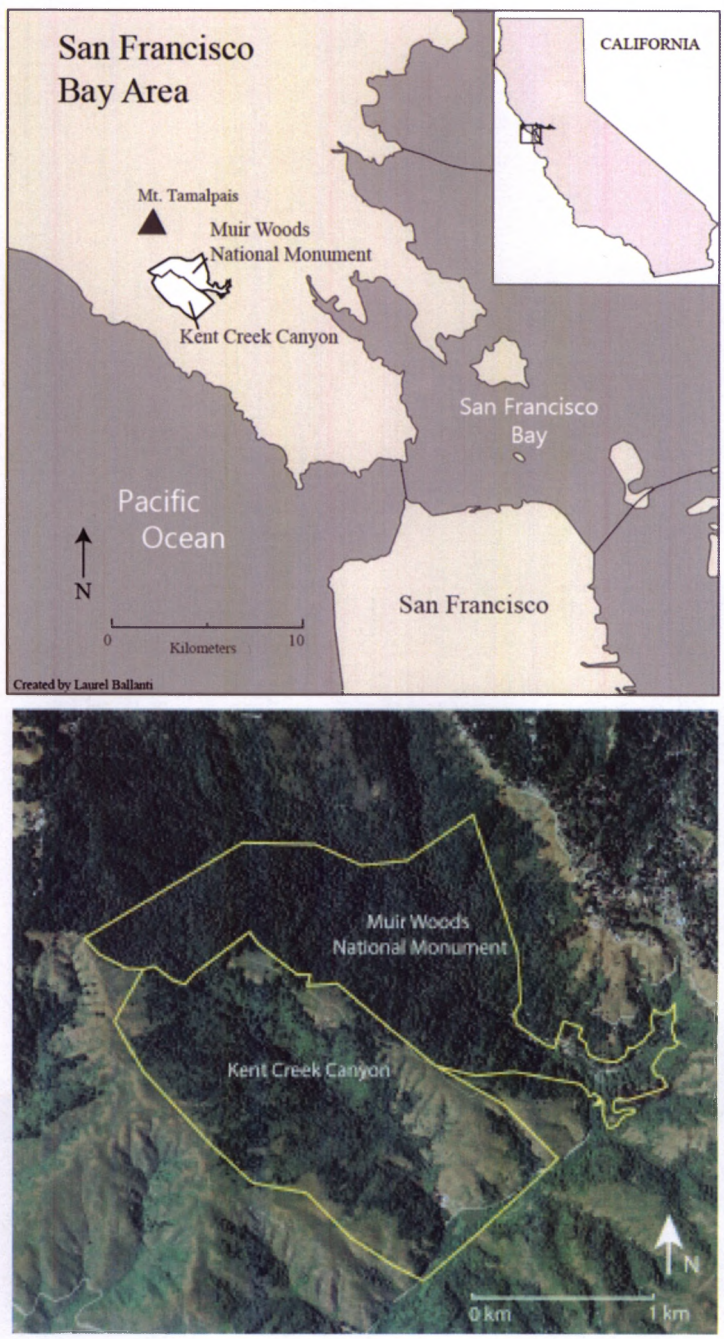

Figure 1: Muir Woods National Monument and Kent Creek Canyon are located along the California coastal range in the San Francisco Bay Area.

To the west of Muir Woods National Monument is the smaller Kent Creek Canyon, part of Mt. Tamalpais State Park. The Kent Creek area exhibits drier conditions than Redwood Canyon. In this area, bay laurel and coast live oak (*Querus agrifolia*), and Douglas fir are more abundant, while the extent of coast redwood is limited. Kent Creek Canyon includes extensive non-forested areas containing coyote brush and grassland. In both parks, arroyo willow (*Salix lasiolepis*) and red alder (*Alnus rubra*) corridors line Redwood Creek, while California buckeye (*Aesculus californica*) is found along Muir Woods Road and around the Muir Woods main parking lot. Within the boundaries of Muir Woods National Monument, a small grove of non-native eucalyptus (*Eucalyptus globulus)* sits in the eastern edge of the park in the Canyon de Camino area. The eucalyptus grove was planted before the land was acquired as part of the park (National Park Conservation Association, 2011)

3. Methods

3.1. Remote Sensing Data

Acquisition of remote sensing data for this project occurred through the Golden Gate LiDAR Project (Table 1). Airborne hyperspectral data were acquired using an AISA Eagle sensor with a 23mm lens. The sensor was flown at an altitude of 2286 meters with a FWHM (bandwidth) of approximately 4.6 nm. Multiple flight lines were flown, out of which four flight line images were ultimately selected based on time of day taken, spatial coverage of the study area, and temporal proximity between images. The LiDAR and hyperspectral data were acquired concurrently and an additional flight over Muir Woods National Monument resulted in a LiDAR point density of 4 points/m^2 (Stephen, 2013).

Table 1: After the Minimum Noise Fraction Transform 27 bands were selected to be used in the image classifications. The selection of bands was based on the eigenvalues and percentage of data variance, along with visual inspection of each band.

Data	Sensor	Date of acquisition	Pixel Size	Spectral Range	Bands
Hyperspectral	AISA Eagle	5/5/2010-5/7/2010	2m	397.78-997.96 nm	128
LiDAR	Leica ALS60	5/5/2010-5/7/2010	4pt/m^2		1

3.2. Pre-Processing

The LiDAR point data were classified into ground, canopy and building points, and QA/QC (quality assurance/quality control) was completed to remove noise points using LP360 software (QCoherent, 2014). A 0.5m spatial resolution digital elevation model (DEM) and canopy height model (CHM) were created from the LiDAR data using open source software (GRASS Development Team, 2014).

Most initial pre-processing of the hyperspectral data occurred separately to this study as part of the Golden LiDAR project. Such processing included radiometric corrections from digital numbers to reflectance, geometric calibration, and orthorecification (Stephen, 2013). Additional processing was completed using ENVI 5.1 (Exelis Visual Information Solutions, 2013). Atmospheric corrections were applied to each flight line image using the fast line-of-sight atmospheric analysis of spectral hypercubes (FLAASH) algorithm, converting the image value from radiance to reflectance. Subsets of the hyperspectral flight lines were selected to eliminate edge effects. The four flight line images were then mosaicked using the seamless mosaic tool and histogram matching was applied for normalization. This yielded a hyperspectral mosaic of the study area with 2m spatial resolution. The hyperspectral mosaic finally had a nearest neighbor resampling applied to match the 0.5m spatial resolution of the of the LiDAR data.

3.3. Masking

The study area contains sections of low-lying vegetation and roads which were not considered in the classification. A CHM mask was created and applied to the hyperspectral mosaic, removing any areas below 2 meters from the image. As suggested by Ghosh et al. (2014), a mask was applied to the hyperspectral mosaic to remove non-forest area, reducing the spectral influence of non-tree classes in the principal components during feature selection.

3.4. Object-based tree segmentation

The goal of the object-oriented segmentation approach was to delineate object areas that would include individual tree crowns to be used in the species classification. To aid in the segmentation, tree stems were located by isolating maximum heights based on LiDAR points. When locating tree stems, an assumption was made that all trees take similar form as conifers, with crowns forming a pointed top. While this assumption helped predict tree stem location of coniferous trees, it is likely that other species tree stems were not as readily identified using this method. As a result of this potential error, the tree center locations were used only as a visual guide for the segmentation. eCognition 9.1 software (Trimble, 2015b) was used for segmentation based on the CHM. The multi-resolution segmentation assesses single pixels and combines them with

neighboring pixels based on factors of homogeneity to create object. The three parameters used to tune the segmentation included scale parameter, to adjust the size of objects; shape, to determine the influence of shape verses color; and compactness, which influences the value of compactness over smoothness (Trimble, 2015). To compare the influence of object size on classification accuracy, two segmentations were created, one containing smaller objects, and one with larger objects (Figure 2).

The small object segmentation resulted from a scaling parameter of 6, shape of 0.3, and compactness of 0.8 using trial and error. These parameters increased the likelihood that a tree stem point was contained within a single object while maintaining small object size. This approach, however, resulted in an over-segmentation of objects in some areas. The large object segmentation parameters were also determined using trial and error, resulting in a scaling factor of 9, shape of 0.1 and compactness of 0.5. Visually, the large object delineation aligned closer to actual tree boundaries of the CHM. In some cases, however, the image was under-segmented in areas where merged tree crowns had similar heights.

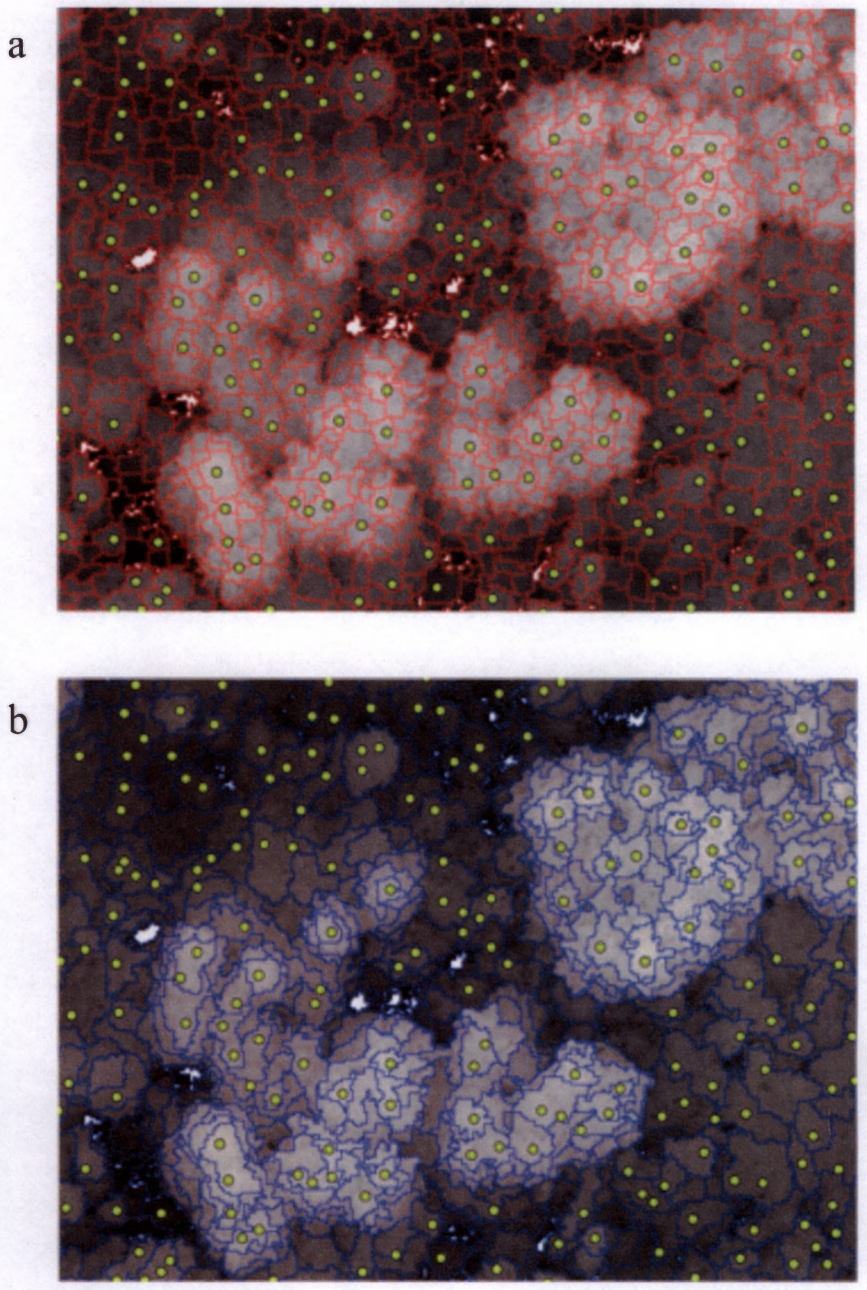

Figure 2: The small segmentation (a) created by the multi-resolution segmentation in eCognition 9.1 displayed over the canopy height model. Points represent tree centers. Over-segmentation is visible. The large segmentation (b) created by the multi-resolution segmentation shows areas of under-segmentation of merged tree crowns.

3.5. Data Reduction and Feature Selection

To address the problem of high data dimensionality in hyperspectral images, a forward minimum noise fraction transform was applied to the mosaicked image to reduce data redundancy and help identify bands containing the most variance. This process creates outputs of uncorrelated bands which are ranked from highest eigenvalue (with most meaningful bands) to lowest eigenvalue (containing noise-filled bands). Due to the masking of low-lying vegetation, the resulting set of MNF bands was ranked only based on variance within forested areas only. A total of 27 features were selected to be used in the final classification, based on visual inspection of the MNF band outputs and the ranked eigenvalues provided (Table 2).

Table 2: After the Minimum Noise Fraction Transform 27 bands were selected to be used in the image classifications. The selection of bands was based on the eigenvalues and percentage of data variance, along with visual inspection of each band.

MNF	Eigenvalue	Percent	MNF	Eigenvalue	Percent
1	1769.69	55.56%	**15**	12.60	72.15%
2	148.59	60.23%	**16**	12.05	72.53%
3	79.96	62.74%	**17**	11.37	72.89%
4	56.29	64.51%	**18**	10.97	73.23%
5	51.37	66.12%	**19**	10.02	73.55%
6	31.97	67.12%	**20**	9.48	73.84%
7	27.03	67.97%	**21**	9.07	74.13%
8	21.76	68.65%	**22**	8.90	8.9096
9	21.35	69.33%	**23**	8.87	74.69%
10	19.37	69.93%	**24**	8.79	74.96%
11	16.71	70.46%	**25**	8.73	75.24%
12	14.09	70.90%	**26**	8.66	75.51%
13	13.95	71.34%	**27**	8.59	75.78%
14	13.28	71.76%			

3.6. Sample Data

Stratified random sampling was used to select both training and testing samples for the classification. Single species tree stands were used as strata to reduce potential error when identifying a tree sample, and to remove the possibility of mixed-species pixels. Field work consisted of navigating to pre-selected random points within stands using GPS and a detailed CHM to confirm the species of the tree at each point. Given the steep terrain and thick vegetation in the study area, samples that could not be checked in the field where confirmed using high resolution reference imagery. From the total samples collected, a points were randomly assigned into training and testing samples. Training sample polygons were manual drawn around the training sample points with CHM tree crowns as a guideline.

To determine the number of training pixels needed for each class, a common rule suggests multiplying the number of bands used in the classification by ten (McCoy, 2005). Given the object-based approach used in this research, this rule was used as a guideline to create both small and large training sample sizes to understand the influence of training sample size on the two classifiers (Table 3). The small training sample set was based on the training sample polygons, where the value of the sample equaled the mean spectral value of the pixels within the polygon. The same training sample polygons were used in the large training sample set, however, each pixel contained within the polygon was used as a training sample. All samples were proportionally selected for each class.

Table 3: Training and testing samples by class. A total of 806 samples were collected (Small training sample set and testing samples.) The large training sample set utilized all pixels within the sample polygons as training samples. [1]Estimated percent coverage was calculated from an initial unsupervised classification of the study area.

Class	Percent Coverage [1]	Small Training Sample Size	Large Training Sample Size	Testing Sample Size
Arroyo Willow *(Salix lasiolepis)*	1.0%	10	139	19
California Bay Laurel *(Umbellularia californica)*	26.2%	27	371	152
California Buckeye *(Aesculus californica)*	0.1%	12	180	15
Coast Live Oak *(Querus agrifolia)*	5.1%	16	192	30
Coast Redwood *(Sequoia semperviren)*	40.0%	24	254	276
Douglas Fir *(Pseudotsuga menziesii)*	26.0%	25	236	135
Eucalyptus *(Eucalyptus globulus)*	0.5%	23	134	10
Red Alder *(Alnus rubra)*	1.10%	16	201	26
Total	100%	143	1707	663

The number of test samples needed for accuracy testing were based on the multinomial distribution for a confidence interval of 90% for the accuracy assessment (Congalton & Green, 2008). Although a confidence interval of 95% would have been preferred, the number of test samples required to attain that level was beyond the scope of this project, especially given the hard to access terrain. Testing samples for each species were also proportionally selected by class size. A total of 663 test samples were determined necessary for a confidence interval of 90%.

3.7. Classification

Eight tree species were used in the classification, including coast redwood (*Sequoia sempervirens*), Douglas fir (*Pseudotsuga menziesii*), California bay laurel (*Umbellularia californica*), coast live oak (*Querus agrifolia*), red alder (*Alnus rubra*), arroyo willow (Salix lasiolepis), eucalyptus (Eucalyptus globulus), and California buckeye (*Aesculus californica*). These species were selected based on their estimated percent coverage in the study area, as well as visibility in the canopy.

A comparative classification approach was taken to compare the support vector machine with RBF classifier and the random forest classifier. Additionally, classifications were compared based on the size of the object-oriented segmentation and training samples. The classifier comparisons were divided into a total of 4 classification sets, resulting in eight total classifications, explained below (Table 4).

Table 4: Classification set based on classifier, training sample size, and segmentation size.

Classification Set	Training Sample Size	Segmentation Object Size
Classification Set 1 SVM and RF	*Small sample*	*Small object*
Classification Set 2 SVM and RF	*Small sample*	*Large object*
Classification Set 3 SVM and RF	*Large sample*	*Small object*
Classification Set 4 SVM and RF	*Large sample*	*Large object*

All species classifications were performed using eCognition 9.1 Developer software (Trimble, 2015). A grid search to determine optimal parameters for the SVM and random forest classifiers was completed in R-project (R Core Team 2015) with package 'e1071' (2014). The SVM classifier parameters selected include gamma, which controls the smoothness of the hyperplane, and C, which controls the error penalty (Melgani & Bruzzone, 2004). The RF parameters include m, the number of features used for training, and N, the number of trees. A framework of the steps for these methods can be found in Figure 3.

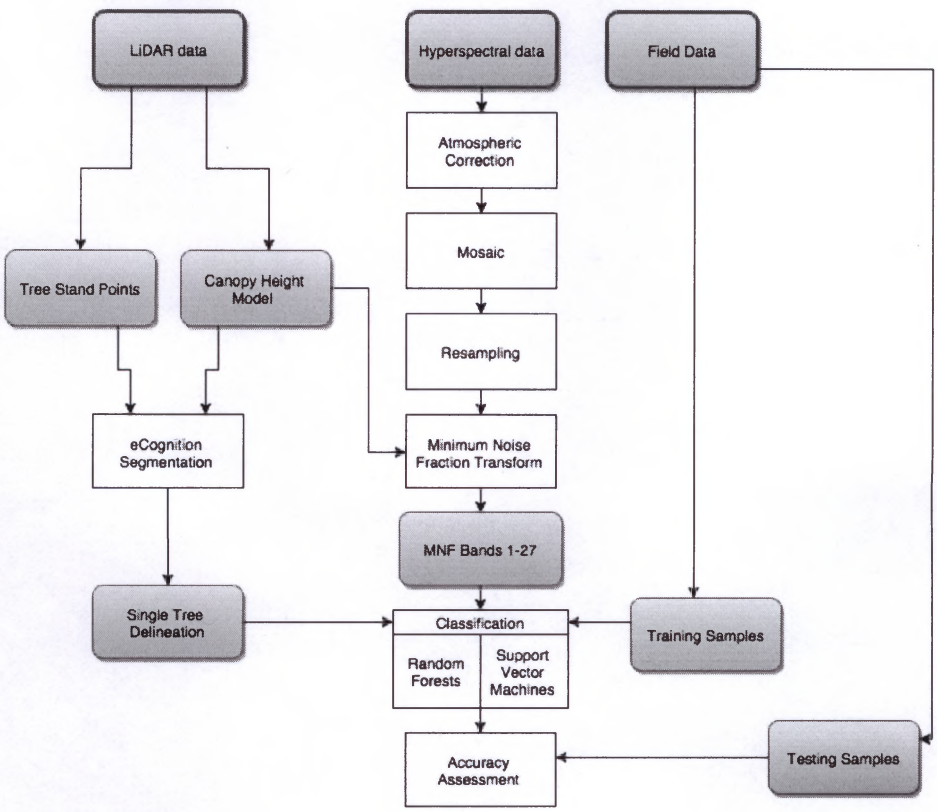

Figure 3: Framework of the tree species classification using LiDAR, hyperspectral, and field data.

3.8. Accuracy Assessment

A visual inspection of each classification was performed to identify areas of potential error and contrast between classifications. Also, the results of the classifications were assessed according to the confusion matrix based on overall accuracy, Kappa coefficient, user's accuracy, and producer's accuracy (Congalton, 1991).

McNemar's test has been frequently used for testing the statistical significance of two classifiers (Tarabalka et al., 2010; Jones et al., 2010; Pal & Foody, 2010; and Ghosh et al., 2014). Foody (2004) suggests the use of McNemar's test instead of a z-test in cases where the same test samples are used for each accuracy assessment, resulting in the assumption of independence of samples to not be fulfilled. The McNemar's test (Everitt, 1977) measures the error of two proportions that use the same training sample set, where the null hypothesis assumes that the error produced by each classifier is the same (Dietterich, 1998). For this research, the McNemar's test was used to determine if differences in accuracies between the SVM and RF classifier were statistically significant, as well as any change in performance of the individual classifiers when training and segmentation sizes are adjusted. The confidence interval for statistical testing was 95%.

4. Results

4.1. Classification Set 1: Small training sample size, small segmentation

In classification set 1, SVM and RF classifiers were assessed using a small training sample size to classify the small object-based segmentation. A grid search resulted in the selection of optimal parameters for SVM, where gamma = 16 and C = 0.00781, and RF, where m = 5 and N = 2000.

In a visual assessment of the two classifications, the random forest classifier resulted in a less homogeneous classification of species than the support vector machine classifier (see Appendix 2 for classification). Specifically, the redwood grove on the western edge of Kent Canyon contained more coast live oak and buckeye in the RF classification (Figures 4). Additionally, in the upper right corner of the study area, RF classified multiple areas red alder and eucalyptus, while both classifiers identified coast live oak within Douglas fir stands (Figures 5). Both classifiers identify Douglas fir along redwood creek in the lower portion of the image, despite this species not being found in that area. Similarly, both classifiers misclassified coast live oak and Douglas fir as willow and red alder on the outer edges of the forests on non-riparian hillsides.

The SVM classification resulted in an Overall Accuracy (OA) of 92.61% and the RF classifier resulted in an OA of 91.55% (Table 5).

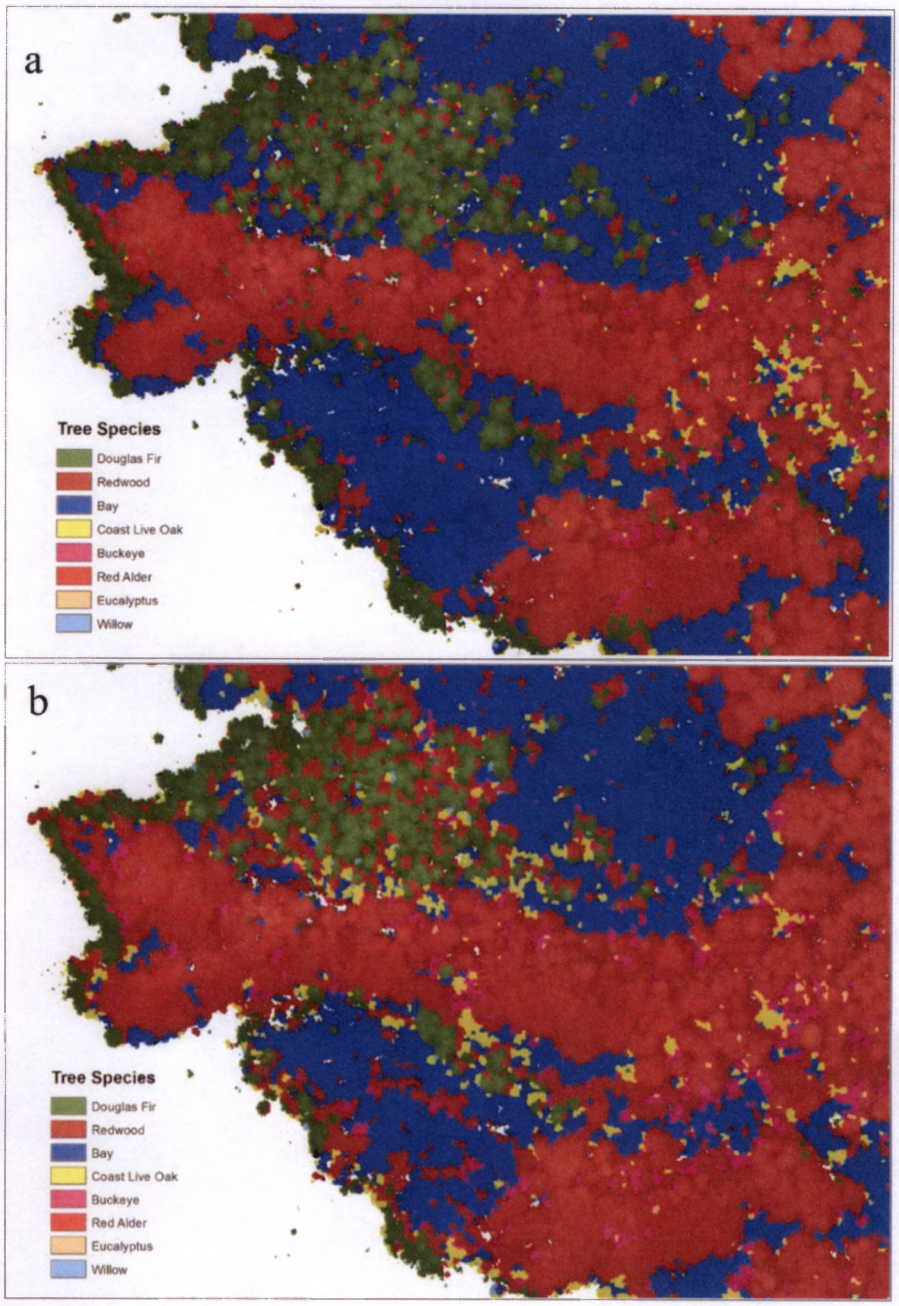

Figure 4: A portion of the support vector machine classification (a) with buckeye and coast live oak occurring less frequently than in the RF classification (b). Douglas fir and bay stands contain more class variation in the RF classification.

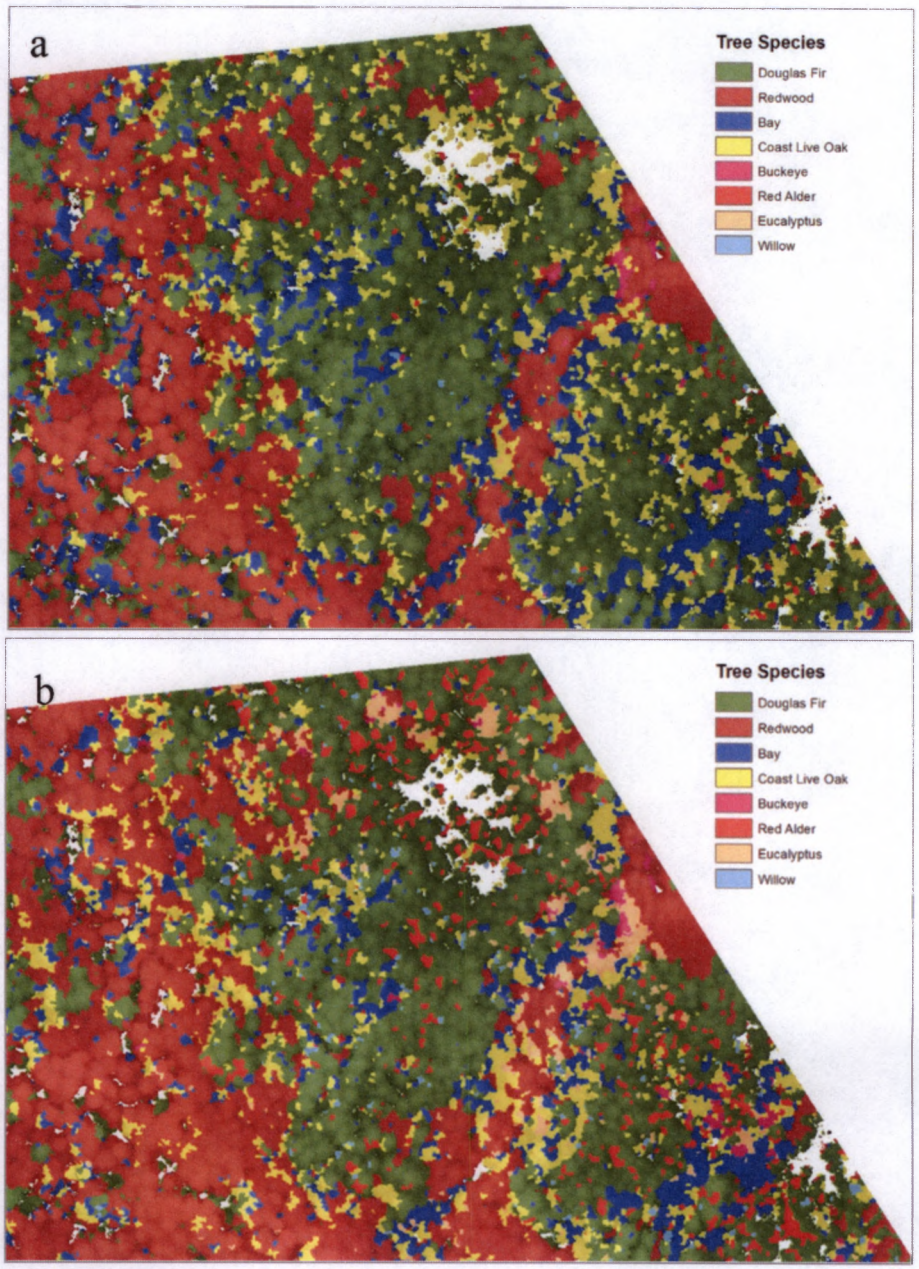

Figure 5: The eastern edge of the support vector machine classification (a) from classification set 1 shows a mix of redwood, bay, coast live oak, and Douglas fir. The random forest classification (b) from set 1 shows increased coast live oak and abundant red alder, compared to the SVM classification.

Table 5: Statistical significance of the classification sets.

Classification Set	Classifier	Overall Accuracy	P-value	Statistical significance
Classification Set 1	SVM	92.61%	.3408	Not significant
	RF	91.55%		
Classification Set 2	SVM	92.76%	.4404	Not Significant
	RF	92.31%		
Classification Set 3	SVM	94.72%	.0119	**Significant**
	RF	92.46%		
Classification Set 4	SVM	95.02%	.0164	**Significant**
	RF	92.91%		

Although neither classifier statistically outperformed the other, there was some variety in the success of classifying certain species (see Appendix 1 for confusion matrices). Both classifiers resulted in a low producer's accuracy of 57.89% for willow. For the SVM classifier, the three additional species resulting in moderate producer's accuracies were coast live oak (80.00%), buckeye (80.00%), and eucalyptus (70.00%). User's accuracies for all species in the SVM classification, except coast live oak (63.16%), were above 88.81%. For the RF classification, buckeye resulted in a low producer's accuracy of 66.66%, while coast live oak and red alder demonstrated low user accuracy of 68.42% and 70.97%. The biggest contrasts between classifier accuracies were with eucalyptus (SVM: user's accuracy of 100.00%, producer's accuracy of 70.00%; and RF: user's accuracy of 81.82%, producer's accuracy of 90.00%), and red alder (SVM: user's accuracy of 91.67% and RF user's accuracy of 70.97%). Classification accuracies for bay and redwood were consistently high (above 92%) for both classifiers.

4.2. Classification Set 2: Small training sample size, large segmentation

This set of classifications examined the use of a small training sample set applied to the larger object-based segmentation. A grid search resulted in the same parameters as the previous classification set.

In a visual inspection of the two classifications, coast live oak was classified more abundantly among the redwood and Douglas fir in the upper areas of the mosaic in the RF classification than in the SVM classifier (see Appendix 3). In the RF classification, red alder and eucalyptus remain on the right side of the image, though less abundantly than in classification set 1. The SVM classification had fewer pockets of isolated redwood in the Kent Canyon area, resulting in the appearance of a more generalized and homogenous classification.

Overall accuracy for the SVM classification was 92.76% and the accuracy for RF was 92.31% (Table 5).

The classification of individual species resulted in high accuracies for most species with each classifier. SVM user's accuracies were all above 80%, although many exceeded 90%. All but two classes, willow (57.89%) and coast live oak (76.87%), were 80% or higher for producer's accuracy. RF generally resulted in class accuracies above 80%, except for coast live oak and red alder with user's accuracies of 61.54% and 75.00%, and willow with a producer's accuracy of 52.63%.

4.3. *Classification Set 3: Large training sample size, small segmentation*

For classification set 3, training sample size was increased by including reflectance values of all pixels within the training polygons. As a result, a new grid search for parameter selection was performed for each classifier resulting in gamma = 16 and C = .0156 for SVM, and m = 10 and N = 2000 for RF.

A visual comparison of the two classifications highlights the increasing homogeneity of species stands in the SVM classification over the RF classification (see Appendix 4). The classification of red alder and eucalyptus in the upper right corner in the RF classification was less defined than in classification sets 1 and 2. The RF classifier misidentified a portion of the eucalyptus grove in the upper right corner of the study area as redwood, while the SVM identified it as solely eucalyptus. Similarly, the presence of Douglas fir along Redwood creek was reduced in the SVM classification, but not with the RF classification.

The classification accuracies of the large training samples resulted in an OA of 94.72% for the SVM classifier and an OA of 92.40% for the RF classifier (Table 5). The difference in accuracies was found to be significant.

In the classification of individual species certain species stand out with less than ideal performance. As with all previous classifications, willow resulted in a low producer's accuracy (57.89%) for both classifiers. Unlike the other classifications, user's

accuracy for red alder increased by more than 10% to 88.46% with the RF classifier, although SVM continued to have a high user's accuracy (95.85%) for red alder. In the SVM classification, the user's accuracy for buckeye decreased with the large training samples when compared the small training sample classifications. Coast live oak continued to result in low user's accuracy, while bay and redwood continued to have high accuracies for both classifiers.

4.4. Classification Set 4: Large training sample size, large segmentation

This classification set used the large training sample set to classify the large object segmentation. The SVM parameters were a gamma of 16 and cost of 0.0156, while the RF parameters had an m of 5 and N of 2000.

In these classifications the improvement in overall accuracies was consistent with the visual improvement of the classification images (see Appendix 5). As in the previous classifications, RF continued to identify redwood trees in the eucalyptus grove and Douglas fir along Redwood Creek when the SVM classification did not. Similar to previous RF classifications, red alder was identified along the right edge of the image, however the eucalyptus was not as distinct as with previous RF classifications. Both classifications had a decrease in species heterogeneity with the increase of training samples and larger segmentation.

The overall accuracy for the SVM was 95.02% and OA for RF was 92.91% (Table 5). The advantage of the SVM classifier over the RF classifier was significant. Additionally, the classification set 4 resulted in the highest overall accuracies for both classifiers (Table 6).

For individual class accuracies, both classifiers resulted in a 57.89% producer's accuracy for willow. The RF classifier resulted in willow user's accuracy dropping by at least 10% from previous classifications. The RF classifier user's accuracy for coast live oak remained low at 62.50%, while SVM user's accuracy for coast live oak went from below 75% in all previous classifications to 90.32%. Aside from coast live oak and willow, both classifiers had producer's and user's accuracy above 90% for all other species.

Table 6: Confusion matrices for classification set 4, which resulted in the highest overall accuracies for both classifiers. The top row of classes represents the reference trees and the left column represents classified trees.

SVM	DF	RW	Bay	CLO	BU	RA	E	W	Total	User's Accuracy
DF	126	4	1	2	1	1	0	3	138	91.30
RW	0	271	1	0	0	0	0	0	272	99.63
Bay	1	0	147	0	0	0	0	0	148	99.32
CLO	6	1	3	28	0	0	1	3	42	66.67
BU	0	0	0	0	14	0	0	1	15	93.33
RA	1	0	0	0	0	24	0	1	26	92.31
E	0	0	0	0	0	0	9	0	9	100.00
W	1	0	0	0	0	1	0	11	13	84.62
Total	135	276	152	30	15	26	10	19	663	
Producer's Accuracy	93.33	98.19	96.71	93.33	93.33	92.31	90.00	57.89		
Overall Accuracy	**95.02**									
Kappa	**0.931**									

DF- Douglas fir, RW- Redwood, Bay- Bay, Coast Live Oak- CLO, Buckeye- BU, RA- Red Alder, E- Eucalyptus, W-Willow

RF	DF	RW	Bay	CLO	BU	RA	E	W	Total	User's Accuracy
DF	117	3	1	3	0	0	0	2	126	92.86
RW	3	272	2	1	0	0	1	0	279	97.49
Bay	4	1	146	1	0	0	1	0	153	95.42
CLO	6	0	3	25	1	1	0	4	40	62.50
BU	0	0	0	0	14	0	0	1	15	93.33
RA	3	0	0	0	0	23	0	1	27	85.19
E	0	0	0	0	0	0	8	0	8	100.00
W	2	0	0	0	0	2	0	11	15	73.33
Total	135	276	152	30	15	26	10	19	663	
Producer's Accuracy	86.67	98.55	96.05	83.33	93.33	88.46	80.00	57.89		
Overall Accuracy	**92.91**									
Kappa	**0.902**									

DF- Douglas fir, RW- Redwood, Bay- Bay, Coast Live Oak- CLO, Buckeye- BU, RA- Red Alder, E- Eucalyptus, W-Willow

4.5. Classifier performance

The performance of both the SVM and RF classifiers were also assessed individually to determine if the size of training samples, segmentation size, or both, would change the performance of a classifier. The increase in segmentation size alone did not improve the SVM or RF classifications with any significance. The addition of training samples improved the SVM overall accuracy for both the small segmentation and large segmentation with p-values of 0.0258. With a confidence interval of 95%, the improvement of the SVM classifier can be considered significant.

The increase of both training sample size and the larger object size together resulted in higher overall classification accuracies for the two classifiers. The SVM performance in classification set 1 (92.61% OA) and the performance of SVM in classification set 4 (95.02%) was statistically significant with a p-value of 0.0058. Similarly, the increase in overall accuracy for the random forest classifier from set 1 (91.55%) to set 4 (92.91%) was statistically significant, with a p-value of 0.0425.

5. Discussion

In comparing the overall accuracies of the SVM and RF classifier, SVM was determined to have a statistically significant advantage over RF when the number of training samples were increased, irrespective of segmentation size. The most misclassified class for both classifiers was willow, with class accuracies all below 60%. The willow class was misclassified as multiple different species, with coast live oak being the most common. Redwood most consistently had the fewest misclassifications.

A noticeable trait of both classifiers was the generally high overall accuracies despite abundant misclassifications identified during visual inspection. Duro et al. (2012) experienced similar issues with their classification, highlighting that limited testing samples can result in inaccurate classification accuracies. Similarly, Congalton (1991) explains that a large quantity of zeroes within the confusion matrix can mean that the test sample size is inadequate, or the classification highly successful. Considering the number of zeroes on the confusion matrix for the smaller classes (eucalyptus, willow, coast live oak, etc.), it is quite possible that insufficient test samples were responsible for the high classification accuracies of some species. For this research, the stratified sampling method utilized single species stands to ensure correct sample identification, however, this prevented test samples from being selected near stand boundaries, in mixed forest areas, or in inaccessible areas. As a result, the test samples did not represent all areas of

the study site, and thus the accuracy assessment failed to reflect the classifier performance in those areas.

In some cases, an individual species was misclassified as one or two other classes, as was demonstrated by the redwood class commonly being incorrectly classified as bay or Douglas fir. As discussed by Heinzel & Koch (2012), misclassification within the same tree types (conifers and broadleaf) occur at a higher rate than they do between tree types. Some broadleaf tree classes (coast live oak, buckeye, red alder) were misclassified as other broadleaf species, likely as a result of similar spectral signatures among the broadleaf species. The fact that Douglas fir and willow were misclassified as many different species of various tree type, however, may suggest a different cause of some misclassifications. Leckie et al. (2005) highlight the causes of high spectral variability in old growth forests, which include shadowing, tree health, and bidirectional reflectance. Shadowing may best explain the misclassification of Douglas fir as coast live oak in the found throughout the upper portions of the mosaic. Additionally, sun angle and slope can change reflectance values based on date and time of day. Although a normalization was applied to the images before mosaicking, the normalization was likely insufficient for the non-consecutive flight lines. Because training samples from all images were used to train the classifiers, the result was a wider spectral range for some classes, causing spectral overlap which leads to misclassification of species.

The influence of training sample size played a significant role in the SVM and RF classifications. For both the small and large segmentations, the increase in training samples improved the SVM classification to the point of statistically outperforming the RF classification. The support vector machine classifier is often recognized for its ability to work well will limited training samples (Mountrakis et al., 2011). In this case, however, the small set of training samples may have provided insufficient sample data for the SVM classifier. Tarabalka et al. (2010) did encounter an issue with the SVM classifier, noting that classes with low training sample sizes often resulted in low accuracies for that class, which in turn affects the overall accuracy of the classification. The willow class had the fewest number of training samples and consistently had low class accuracies.

Classifications using small segmentations tended to show greater variety of species within stands, which was likely due to shadowing. Small segmentations that that fit entirely within shadowed areas may not have similar spectral properties to sunlit segments of the same class, resulting in a misclassification of shadowed areas. The larger segmentation might include both shadowed and sunlit portions of a tree resulting in a higher chance of being correctly classified. The result of this artifact is a speckled appearance of species on the small segmentation classification and a more uniform display of species on the large segmentation classification. A difference in smoothness or homogeneity was also noted between the SVM and RF classifiers, regardless of segmentation size, which is likely a result of differences between the classifiers. The

increase in segmentation size alone had no statistically significant influence on classification accuracy. Both classifiers did have notable improvement with both larger segmentations and increased training sample.

6. Conclusion

An object-based classification of tree species was performed on a mosaicked hyperspectral image using two commonly used classifiers. Two variables, training sample size and segmentation size, were adjusted to test classifier performance under these different conditions. Neither classifier outperformed the other statistically when a small training sample size was used, regardless of segmentation size. The SVM classifier accuracy did have a statistical advantage over RF when training sample size was increased. The individual performance of the SVM classifier was significantly improved with an increase in training samples. With the addition of training samples and a larger segmentation size, both SVM and RF accuracy had statistically significant improvement. Based on the overall accuracy of the classifications, SVM offers an advantage over RF if sufficient training samples are provided, otherwise no significant difference in performance was found.

Considering the challenging environment of the study area, all classifications successfully resulted in high overall accuracies. The limited accessibility to the study area restricted the number of samples that could be collected, providing additional challenges. Similarly, the sun illumination differences between non-consecutive flight lines, which were enhance by the steep canyons of the study area increased opportunities for misclassifications. Despite these limitations, both SVM and RF maintained high accuracies.

7. References

Akar, Ö., & Güngör, O. (2013). Classification of multispectral images using Random Forest algorithm. *Journal of Geodesy and Geoinformation*, *1*(2).

Alonzo, M., Bookhagen, B., & Roberts, D. A. (2014). Urban tree species mapping using hyperspectral and lidar data fusion. *Remote Sensing of Environment*, *148*, 70-83.

Breiman, L. (2001). Random forests. *Machine learning*, *45*(1), 5-32.

Buddenbaum, H., Schlerf, M., & Hill, J. (2005). Classification of coniferous tree species and age classes using hyperspectral data and geostatistical methods. *International Journal of Remote Sensing*, *26*(24), 5453-5465.

Clark, M. L., Roberts, D. A., & Clark, D. B. (2005). Hyperspectral discrimination of tropical rain forest tree species at leaf to crown scales. *Remote sensing of environment*, *96*(3), 375-398.

Congalton, R. G. (1991). A review of assessing the accuracy of classifications of remotely sensed data. *Remote sensing of environment*, *37*(1), 35-46.

Congalton, R. G., & Green, K. (2008). *Assessing the accuracy of remotely sensed data: principles and practices*. CRC press.

Cutler, D. R., Edwards Jr, T. C., Beard, K. H., Cutler, A., Hess, K. T., Gibson, J., & Lawler, J. J. (2007). Random forests for classification in ecology. *Ecology*, *88*(11), 2783-2792.

Dale, V., Joyce, L., McNulty, S., Neilson, R., Ayres, M., Flannigan, M., Hanson, R., Irland, L., Lugo, A., Peterson, C., Simberloff, D., Swanson, F., Stocks, B., Wotton, B. (2001) Climate Change and Forest Disturbances. *BioScience,* 51 (9), 723-734.

Dalponte, M., Bruzzone, L., & Gianelle, D. (2008). Fusion of hyperspectral and LIDAR remote sensing data for classification of complex forest areas. *Geoscience and Remote Sensing, IEEE Transactions on*, *46*(5), 1416-1427.

Dalponte, M., Bruzzone, L., & Gianelle, D. (2012). Tree species classification in the Southern Alps based on the fusion of very high geometrical resolution multispectral/hyperspectral images and LiDAR data. *Remote sensing of environment*, *123*, 258-270.

Dalponte, M.., Ørka, H. O., Ene, L. T., Gobakken, T., & Næsset, E. (2014). Tree crown delineation and tree species classification in boreal forests using hyperspectral and ALS data. *Remote sensing of environment*, *140*, 306-317.

Denghui, Z., & Le, Y. (2011). Support vector machine based classification for hyperspectral remote sensing images after minimum noise fraction rotation transformation. *Internet Computing & Information Services (ICICIS), 2011 International Conference on* (pp. 132-135). IEEE.

Dietterich, T. (1998). Approximate Statistical Tests for Comparing Supervised Classification Learning Algorithms. *Neural Computations* 10, 1895-1923.

Duro, D. C., Franklin, S. E., & Dubé, M. G. (2012). A comparison of pixel-based and object-based image analysis with selected machine learning algorithms for the classification of agricultural landscapes using SPOT-5 HRG imagery. *Remote Sensing of Environment*, *118*, 259-272.

Trimble. (2015) *eCognition: User Guide 9.1*, Munich, Germany.

Trimble. (2015b) eCognition Developer 9.1 [Computer Software], Munich, Germany.

Everitt, B.S. (1977). The analysis of contingency tables. London: Chapman and Hall.

Exelis Visual Information Solutions. (2013). *ENVI Help*. Boulder, Colorado: Exelis Visual Information Solutions.

Foody, G. (2004). Thematic Map Comparison: Evaluating the Statistical Significance Differences in Classification Accuracy. *Photogrammetric Engineering & Remote Sensing,* 70(5), 627-633.

Franklin, J. (2010). Mapping species distributions: spatial inference and prediction. Cambridge University Press.

Franklin, S. E. (2001). Remote sensing for sustainable forest management. CRC Press.

Franklin, S. E., Hall, R. J., Moskal, L. M., Maudie, A. J., & Lavigne, M. B. (2000). Incorporating texture into classification of forest species composition from airborne multispectral images. *International Journal of Remote Sensing*, *21*(1), 61-79.

Ghosh, A., Fassnacht, F. E., Joshi, P. K., & Koch, B. (2014). A framework for mapping tree species combining hyperspectral and LiDAR data: Role of selected classifiers and sensor across three spatial scales. *International Journal of Applied Earth Observation and Geoinformation*, *26*, 49-63.

Gislason, P. O., Benediktsson, J. A., & Sveinsson, J. R. (2006). Random forests for land cover classification. *Pattern Recognition Letters*, *27*(4), 294-300.

GRASS Development Team, (2014) Geographic Resources Analysis Support System (GRASS) Software, Version 6.4.4. Open Source Geospatial Foundation. http://grass.osgeo.org

Heinzel, J., & Koch, B. (2012). Investigating multiple data sources for tree species classification in temperate forest and use for single tree delineation. *International Journal of Applied Earth Observation and Geoinformation*, *18*, 101-110.

Holmgren, J. Persson, A., & Söderman, U. (2008). Species identification of individual trees by combining high resolution LiDAR data with multi-spectral images. *International Journal of Remote Sensing*, 29(5), 1537-1552.

Hughes G.F., (1968). On the mean accuracy of statistical pattern recognizers, *IEEE Trans. Inform. Theory*, 14, 55-63.

Jones, T. G., Coops, N. C., & Sharma, T. (2010). Assessing the utility of airborne hyperspectral and LiDAR data for species distribution mapping in the coastal Pacific Northwest, Canada. *Remote Sensing of Environment*, 114(12), 2841-2852.

Key, T., Warner, T. A., McGraw, J. B., & Fajvan, M. A. (2001). A comparison of multispectral and multitemporal information in high spatial resolution imagery for classification of individual tree species in a temperate hardwood forest. *Remote Sensing of Environment*, *75*(1), 100-112.

Landgrebe, D. (2002). Hyperspectral Image Data Analysis as a High Dimensional Signal Processing Problem. *IEEE Signal Processing Magazine*, 19(1), 17-28.

Leckie, D. G., Tinis, S., Nelson, T., Burnett, C., Gougeon, F. A., Cloney, E., & Paradine, D. (2005). Issues in species classification of trees in old growth conifer stands. *Canadian Journal of Remote Sensing*, *31*(2), 175-190.

QCoherent (2014) LP360 [Computer Software], Madison, Al.

Martin, M. E., Newman, S. D., Aber, J. D., & Congalton, R. G. (1998). Determining forest species composition using high spectral resolution remote sensing data. *Remote Sensing of Environment*, *65*(3), 249-254.

McCoy, R. M. (2005). *Field methods in remote sensing*. Guilford Press.

Melgani, F., & Bruzzone, L. (2004). Classification of hyperspectral remote sensing images with support vector machines. *Geoscience and Remote Sensing, IEEE Transactions on*, *42*(8), 1778-1790.

Mountrakis, G., Im, J., & Ogole, C. (2011). Support vector machines in remote sensing: A review. *ISPRS Journal of Photogrammetry and Remote Sensing*, *66*(3), 247-259.

National Parks Conservation Association. 2011. State of the Parks, Muir Woods National Monument: A Resource Assessment [last visited 2014 October 22]. Available from: http://www.npca.org/about-us/center-for-parkresearch/stateoftheparks/muir_woods/MuirWoods.pdf

National Park Service. (2008) Muir Woods: 100th Anniversary 2008 [last visited 2014 October 22]. Available from: http://www.nps.gov/muwo/upload/unigrid_muwo.pdf

National Park Service. (2014). Annual Park Recreation Visitation (1904 - Last Calendar Year) Muir Woods NM (MUWO) Reports [Last accessed 015 October 6], Available from: https://irma.nps.gov/Stats/Reports/Park/MUWO

Pal, M., & Foody, G. M. (2010). Feature selection for classification of hyperspectral data by SVM. *Geoscience and Remote Sensing, IEEE Transactions on*, *48*(5), 2297-2307.

Peerbhay, K. Y., Mutanga, O., & Ismail, R. (2013). Commercial tree species discrimination using airborne AISA Eagle hyperspectral imagery and partial least squares discriminant analysis (PLS-DA) in KwaZulu–Natal, South Africa. *ISPRS Journal of Photogrammetry and Remote Sensing*, *79*, 19-28.

R Core Team (2015). R: A language and environment for statistical computing. R Foundation for Statistical Computing, Vienna, Austria. ISBN 3-900051-07-0, URL http://www.R-project.org/.

Rojas, M., Dópido, I., Plaza, A., & Gamba, P. (2010). Comparison of support vector machine-based processing chains for hyperspectral image classification. In *SPIE Optical Engineering+ Applications* (pp. 78100B-78100B). International Society for Optics and Photonics.

Schoenherr, A. A. (1992). *A natural history of California* (Vol. 56). University of California Press.

Shippert, P. (2004). Why use hyperspectral imagery? *Photogrammetric engineering and remote sensing*, *70*(4), 377-396.

Stephen, R. (2013). GGLP SFSU Hyperspectral Processing Report. *University of Victoria- Hyperspectral – LiDAR Research Laboratory.* Print.

Tarabalka, Y., Chanussot, J., & Benediktsson, J. A. (2010). Segmentation and classification of hyperspectral images using watershed transformation. *Pattern Recognition*, *43*(7), 2367-2379.

Van Aardt, J. A. N., & Wynne, R. H. (2007). Examining pine spectral separability using hyperspectral data from an airborne sensor: An extension of field-based results. *International Journal of Remote Sensing*, *28*(2), 431-436.

Voss, M., & Sugumaran, R. (2008). Seasonal effect on tree species classification in an urban environment using hyperspectral data, LiDAR, and an object-oriented approach. *Sensors*, *8*(5), 3020-3036.

Xiao, Q., Ustin, S. L., & McPherson, E. G. (2004). Using AVIRIS data and multiple-masking techniques to map urban forest tree species. *International Journal of Remote Sensing*, *25*(24), 5637-5654.

APPENDIX 1
CONFUSION MATRICES FOR CLASSIFICATION SETS

Classification Set 1

SVM	DF	RW	Bay	CLO	BU	RA	E	W	Total	User's Accuracy
DF	127	4	3	3	2	2	0	2	143	88.81
RW	0	266	0	1	0	0	2	0	269	98.88
Bay	5	5	145	2	0	0	0	0	157	92.36
CLO	3	1	4	24	1	1	1	3	38	63.16
BU	0	0	0	0	12	0	0	1	13	92.31
RA	0	0	0	0	0	22	0	2	24	91.67
E	0	0	0	0	0	0	7	0	7	100.00
W	0	0	0	0	0	1	0	11	12	91.67
Total	135	276	152	30	15	26	10	19	663	
Producer's Accuracy	94.07	96.38	95.39	80.00	80.00	84.62	70.00	57.89		
Overall Accuracy	**92.61**									
Kappa	**0.898**									

DF- Douglas fir, RW- Redwood, Bay- Bay, Coast Live Oak- CLO, Buckeye- BU, RA- Red Alder, E- Eucalyptus, W-Willow

RF	DF	RW	Bay	CLO	BU	RA	E	W	Total	User's Accuracy
DF	118	4	0	2	0	2	0	3	129	91.47
RW	2	267	4	1	0	0	1	0	275	97.09
Bay	7	3	144	1	0	0	0	0	155	92.90
CLO	5	0	4	26	1	0	0	2	38	68.42
BU	0	1	0	0	10	0	0	0	11	90.91
RA	2	0	0	0	4	22	0	3	31	70.97
E	1	1	0	0	0	0	9	0	11	81.82
W	0	0	0	0	0	2	0	11	13	84.62
Total	135	276	152	30	15	26	10	19	663	
Producer's Accuracy	87.41	96.74	94.74	86.67	66.67	84.62	90.00	57.89		
Overall Accuracy	**91.55**									
Kappa	**0.884**									

DF- Douglas fir, RW- Redwood, Bay- Bay, Coast Live Oak- CLO, Buckeye- BU, RA- Red Alder, E- Eucalyptus, W-Willow

Classification Set 2

SVM	DF	RW	Bay	CLO	BU	RA	E	W	Total	User's Accuracy
DF	127	9	3	4	2	2	0	3	150	84.67
RW	1	263	0	0	0	0	1	0	265	99.25
Bay	3	4	147	3	0	0	0	0	157	93.63
CLO	4	0	1	23	0	0	1	2	31	74.19
BU	0	0	0	0	13	0	0	1	14	92.86
RA	0	0	1	0	0	23	0	2	26	88.46
E	0	0	0	0	0	0	8	0	8	100.00
W	0	0	0	0	0	1	0	11	12	91.67
Total	135	276	152	30	15	26	10	19	663	
Producer's Accuracy	94.07	95.29	96.71	76.67	86.67	88.46	80.00	57.89		
Overall Accuracy	**92.76**									
Kappa	**0.900**									

DF- Douglas fir, RW- Redwood, Bay- Bay, Coast Live Oak- CLO, Buckeye- BU, RA- Red Alder, E- Eucalyptus, W-Willow

RF	DF	RW	Bay	CLO	BU	RA	E	W	Total	User's Accuracy
DF	120	4	1	2	0	0	0	2	129	93.02
RW	2	267	3	3	0	0	0	0	275	97.09
Bay	4	2	145	1	0	1	0	0	153	94.77
CLO	7	3	3	24	1	0	0	1	39	61.54
BU	0	0	0	0	12	0	0	1	13	92.31
RA	1	0	0	0	2	24	0	5	32	75.00
E	0	0	0	0	0	0	10	0	10	100.00
W	1	0	0	0	0	1	0	10	12	83.33
Total	135	276	152	30	15	26	10	19	663	
Producer's Accuracy	88.89	96.74	95.39	80.00	80.00	92.31	100.0	52.63		
Overall Accuracy	**92.31**									
Kappa	**0.923**									

DF- Douglas fir, RW- Redwood, Bay- Bay, Coast Live Oak- CLO, Buckeye- BU, RA- Red Alder, E- Eucalyptus, W-Willow

Classification Set 3

SVM	DF	RW	Bay	CLO	BU	RA	E	W	Total	User's Accuracy
DF	129	4	0	3	0	1	0	3	140	92.14
RW	0	270	0	0	0	0	1	0	271	99.63
Bay	2	0	147	0	0	0	0	0	149	98.66
CLO	3	2	5	26	2	1	0	3	42	61.90
BU	0	0	0	1	13	0	0	1	15	86.67
RA	0	0	0	0	0	23	0	1	24	95.83
E	0	0	0	0	0	0	9	0	9	100.00
W	1	0	0	0	0	1	0	11	13	84.62
Total	135	276	152	30	15	26	10	19	663	
Producer's Accuracy	95.56	97.83	96.71	86.67	86.67	88.46	90.00	57.89		
Overall Accuracy	**94.72**									
Kappa	**0.927**									

DF- Douglas fir, RW- Redwood, Bay- Bay, Coast Live Oak- CLO, Buckeye- BU, RA- Red Alder, E- Eucalyptus, W-Willow

RF	DF	RW	Bay	CLO	BU	RA	E	W	Total	User's Accuracy
DF	119	4	0	2	0	1	0	3	129	92.25
RW	1	268	1	1	0	0	2	0	273	98.17
Bay	5	3	147	2	1	0	1	0	159	92.45
CLO	7	0	4	25	1	1	0	3	41	60.98
BU	0	0	0	0	13	0	0	1	14	92.86
RA	2	0	0	0	0	23	0	1	26	88.46
E	0	1	0	0	0	0	7	0	8	87.50
W	1	0	0	0	0	1	0	11	13	84.62
Total	135	276	152	30	15	26	10	19	663	
Producer's Accuracy	88.15	97.10	96.71	83.33	86.67	88.46	70.00	57.89		
Overall Accuracy	**92.46**									
Kappa	**0.896**									

DF- Douglas fir, RW- Redwood, Bay- Bay, Coast Live Oak- CLO, Buckeye- BU, RA- Red Alder, E- Eucalyptus, W-Willow

Classification Set 4

SVM	DF	RW	Bay	CLO	BU	RA	E	W	Total	User's Accuracy
DF	126	4	1	2	1	1	0	3	138	91.30
RW	0	271	1	0	0	0	0	0	272	99.63
Bay	1	0	147	0	0	0	0	0	148	99.32
CLO	6	1	3	28	0	0	1	3	42	66.67
BU	0	0	0	0	14	0	0	1	15	93.33
RA	1	0	0	0	0	24	0	1	26	92.31
E	0	0	0	0	0	0	9	0	9	100.00
W	1	0	0	0	0	1	0	11	13	84.62
Total	135	276	152	30	15	26	10	19	663	
Producer's Accuracy	93.33	98.19	96.71	93.33	93.33	92.31	90.00	57.89		
Overall Accuracy	**95.02**									
Kappa	**0.931**									

DF- Douglas fir, RW- Redwood, Bay- Bay, Coast Live Oak- CLO, Buckeye- BU, RA- Red Alder, E- Eucalyptus, W-Willow

RF	DF	RW	Bay	CLO	BU	RA	E	W	Total	User's Accuracy
DF	117	3	1	3	0	0	0	2	126	92.86
RW	3	272	2	1	0	0	1	0	279	97.49
Bay	4	1	146	1	0	0	1	0	153	95.42
CLO	6	0	3	25	1	1	0	4	40	62.50
BU	0	0	0	0	14	0	0	1	15	93.33
RA	3	0	0	0	0	23	0	1	27	85.19
E	0	0	0	0	0	0	8	0	8	100.00
W	2	0	0	0	0	2	0	11	15	73.33
Total	135	276	152	30	15	26	10	19	663	
Producer's Accuracy	86.67	98.55	96.05	83.33	93.33	88.46	80.00	57.89		
Overall Accuracy	**92.91**									
Kappa	**0.902**									

DF- Douglas fir, RW- Redwood, Bay- Bay, Coast Live Oak- CLO, Buckeye- BU, RA- Red Alder, E- Eucalyptus, W-Willow

APPENDIX 2
COMPARISON OF CLASSIFICATION SET 1
SUPPORT VECTOR MACHINE AND RANDOM FOREST

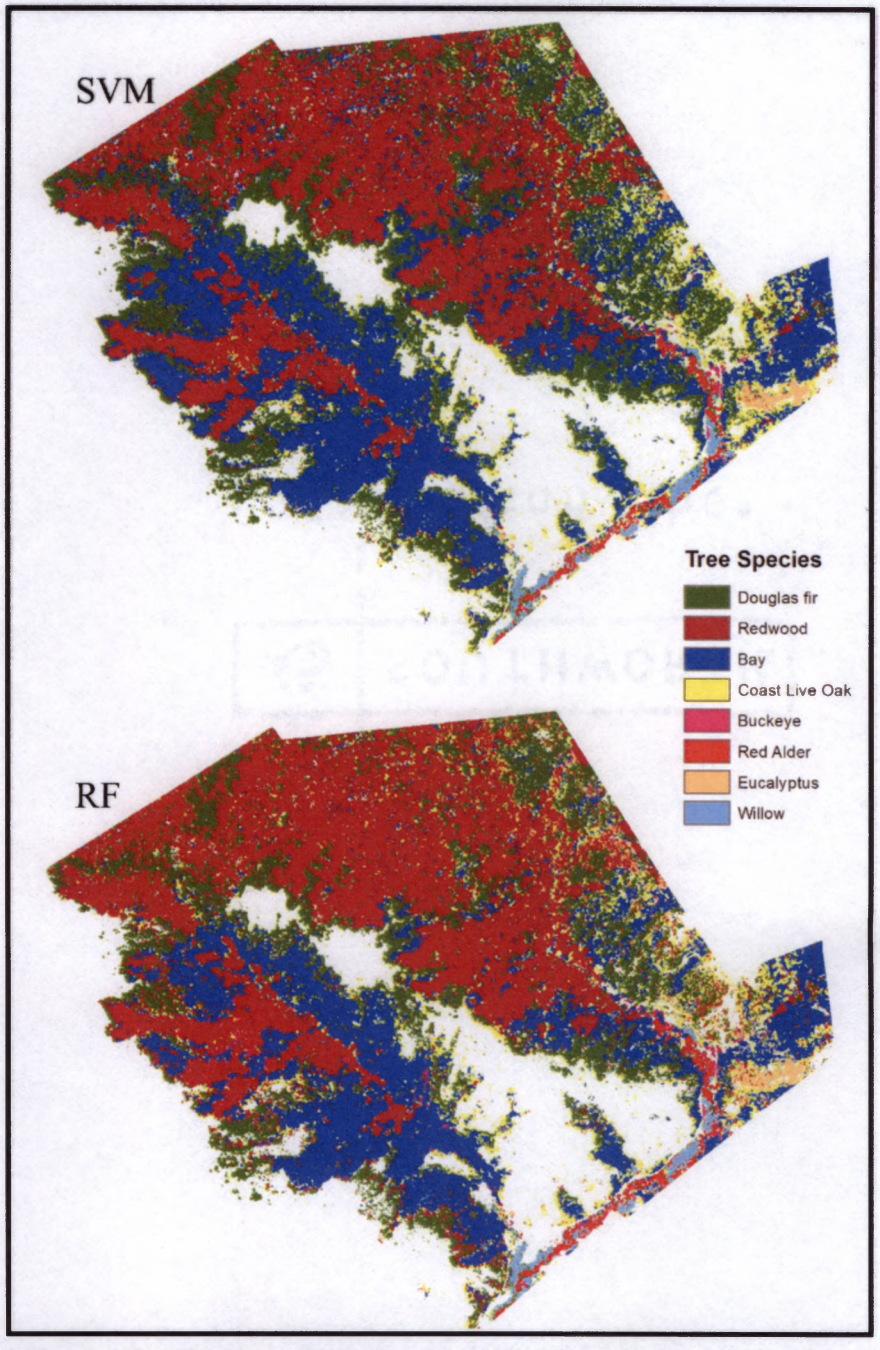

Appendix 2: Species classifications of Muir Woods and Kent Canyon with a small object segmentation and small training sample size using support vector machine classifier (top) and random forest (bottom).

APPENDIX 3
COMPARISON OF CLASSIFICATION SET 2
SUPPORT VECTOR MACHINE AND RANDOM FOREST

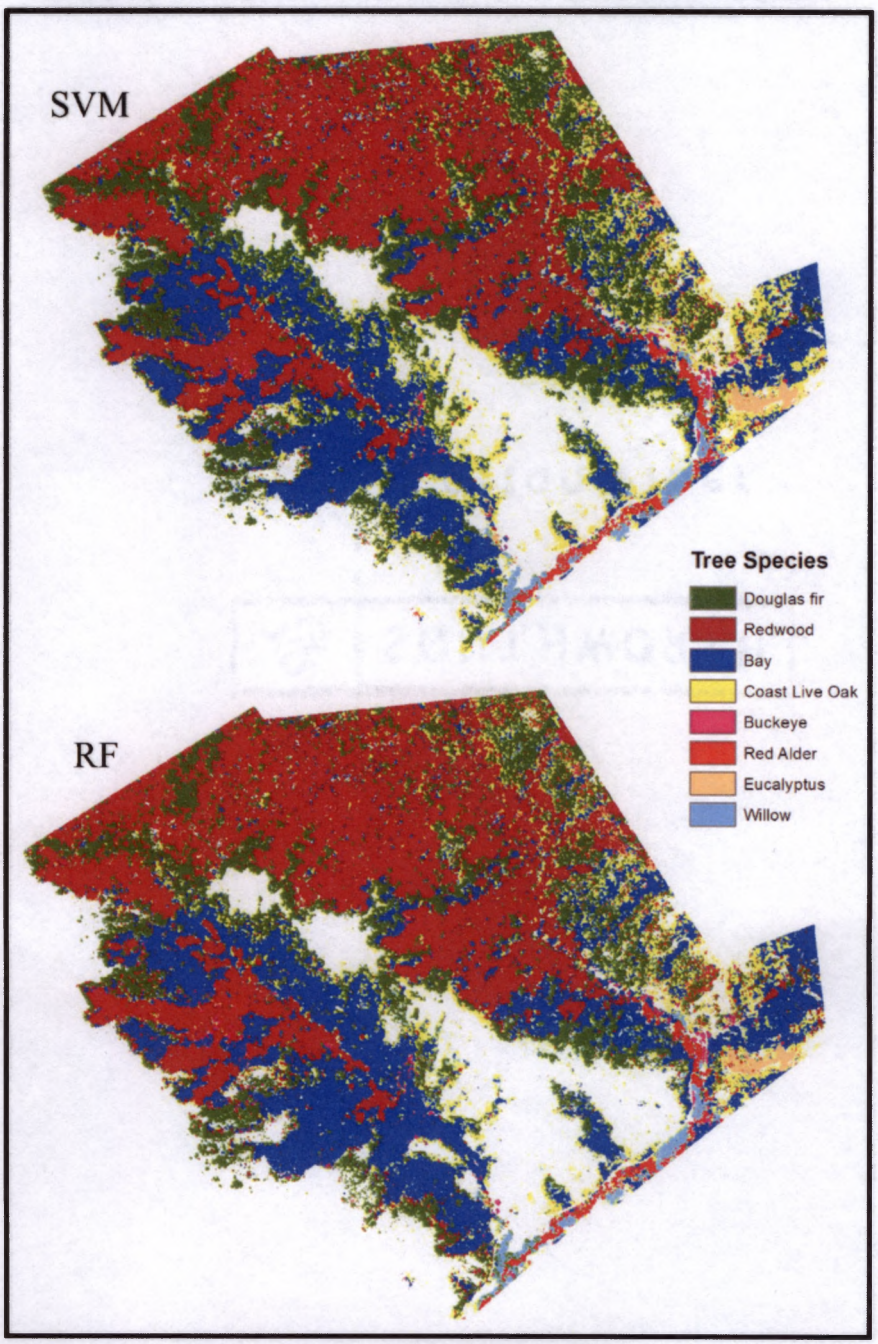

Appendix 3: Species classifications of Muir Woods and Kent Canyon with a small object segmentation and large training sample size using support vector machine classifier (top) and random forest (bottom).

APPENDIX 4
COMPARISON OF CLASSIFICATION SET 3
SUPPORT VECTOR MACHINE AND RANDOM FOREST

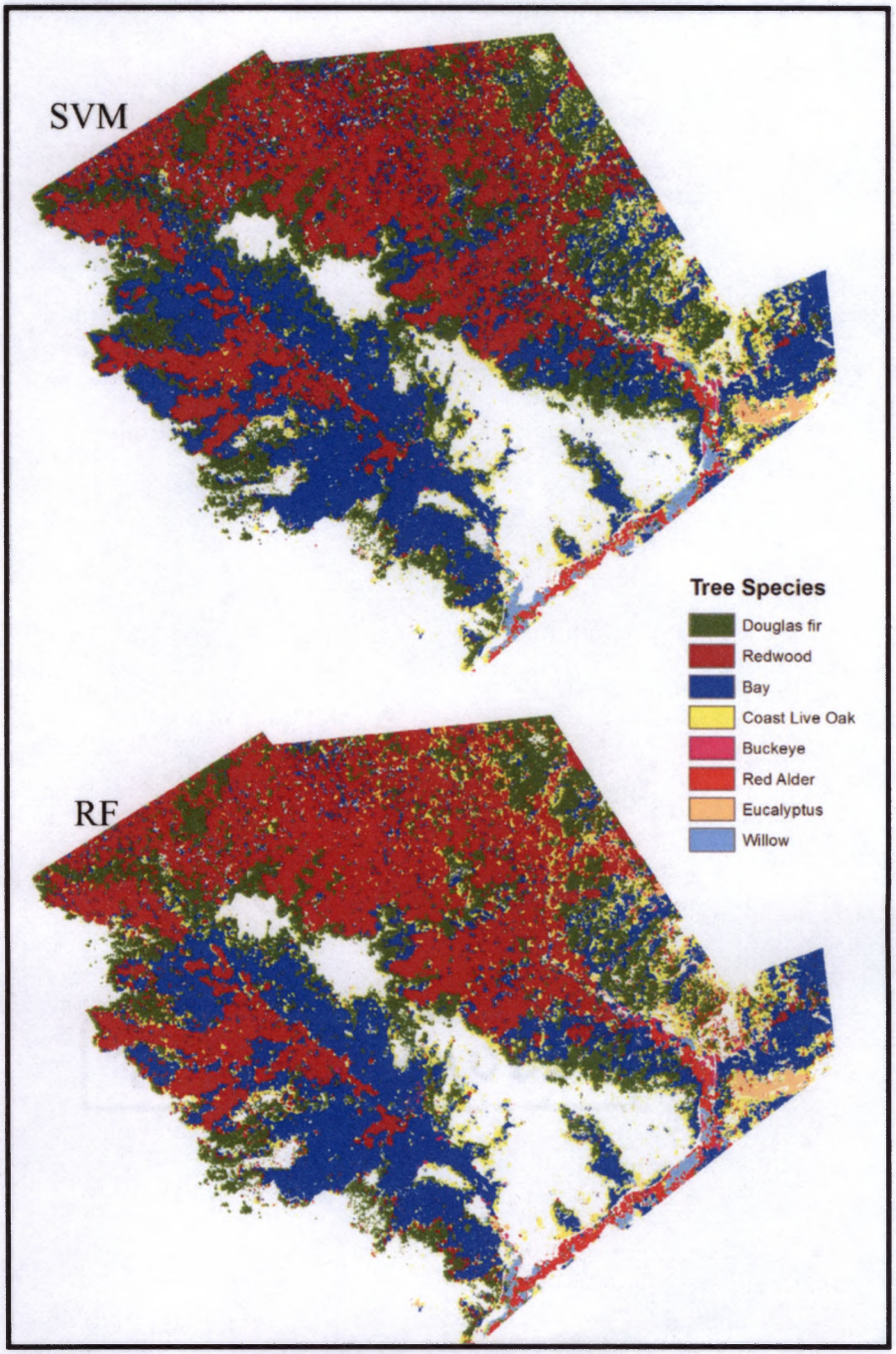

Appendix 4: Species classifications of Muir Woods and Kent Canyon with a large object segmentation and small training sample size using support vector machine classifier (top) and random forest (bottom).

APPENDIX 5
COMPARISON OF CLASSIFICATION SET 4
SUPPORT VECTOR MACHINE AND RANDOM FOREST

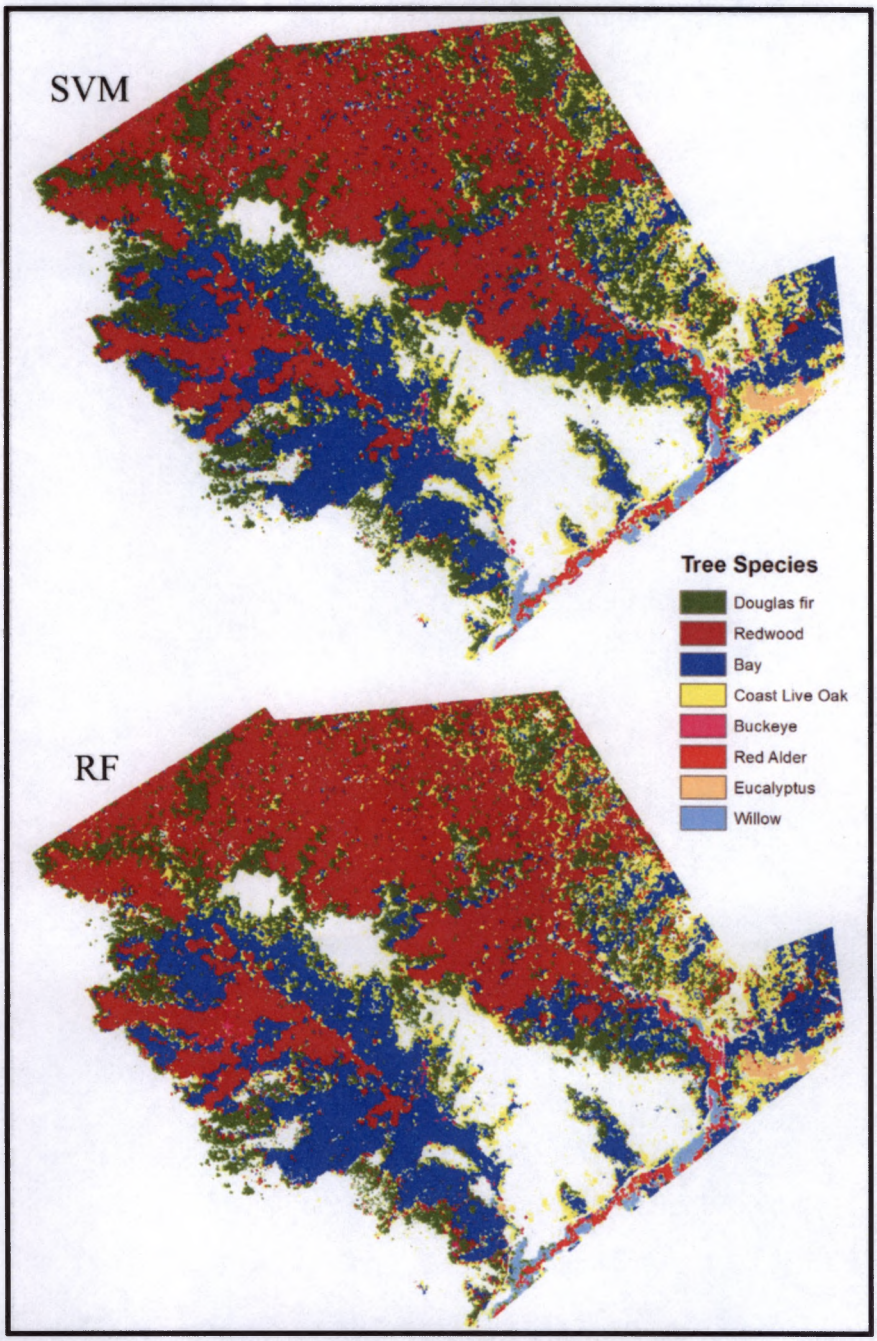

Appendix 5: Species classifications of Muir Woods and Kent Canyon with a large object segmentation and large training sample size using support vector machine classifier (top) and random forest (bottom)